AD_____

GRANT NUMBER DAMD17-96-1-6239

TITLE: Clinical and Technical Performance Evaluation of a Digital Mammography System

PRINCIPAL INVESTIGATOR: Ronald B. Schilling, Ph.D.

CONTRACTING ORGANIZATION: Primex General Imaging Corporation
Carlsbad, California 92008

REPORT DATE: July 1997

TYPE OF REPORT: Annual

PREPARED FOR: Commander
U.S. Army Medical Research and Materiel Command
Fort Detrick, Maryland 21702-5012

DISTRIBUTION STATEMENT: Approved for public release; distribution unlimited

REPORT DOCUMENTATION PAGE

Form Approved
OMB No. 0704-0188

1. AGENCY USE ONLY *(Leave blank)*	2. REPORT DATE	3. REPORT TYPE AND DATES COVERED
	July 1997	Annual (17 Jun 96 - 16 Jun 97)

4. TITLE AND SUBTITLE

Clinical and Technical Performance Evaluation of a Digital Mammography System

5. FUNDING NUMBERS

DAMD17-96-1-6239

6. AUTHOR(S)

Ronald B. Schilling, Ph.D.

7. PERFORMING ORGANIZATION NAME(S) AND ADDRESS(ES)

Primex General Imaging Corporation
Carlsbad, California 92008

8. PERFORMING ORGANIZATION REPORT NUMBER

9. SPONSORING / MONITORING AGENCY NAME(S) AND ADDRESS(ES)

U.S. Army Medical Research and Materiel Command
Fort Detrick, Maryland 21702-5012

10. SPONSORING / MONITORING AGENCY REPORT NUMBER

11. SUPPLEMENTARY NOTES

12a. DISTRIBUTION / AVAILABILITY STATEMENT

Approved for public release; distribution unlimited

12b. DISTRIBUTION CODE

13. ABSTRACT *(Maximum 200 words)*

The goal of the research effort funded under this grant is to finalize the construction of two prototype DXM-1 slot-scanning digital mammography systems, conduct a technical evaluation of these prototypes and perform two clinical studies to assess the efficacy of the systems in the clinical environment. The technical evaluation and one of the clinical studies is being conducted at the Radiology Department at the University of Arizona (UA). The objective of the technical evaluation is to determine system performance parameters such as dynamic range, modulation transfer function, sensitivity, etc. The second clinical study is scheduled to be conducted at Sharp Healthcare/Sidney Kimmel Cancer Center in San Diego, California and will establish the clinical efficacy of the system compared with conventional film/screen mammography. One thousand women are scheduled to participate. Based on preliminary data gathered thus far on the DXM-1 system. The system response is linear with exposure dose and it appears that the dominant noise source is quantum (x-ray) noise. Efforts are now underway to improve system performance by removing artifacts generated in the image reconstruction process, to eliminate parasitic capacitance on the readout IC, and to increase resolution by interleaving both banks of sensors into the displayed image.

14. SUBJECT TERMS	15. NUMBER OF PAGES
Mammography, slot-scan, digital, solid-state	29
	16. PRICE CODE

17. SECURITY CLASSIFICATION OF REPORT	18. SECURITY CLASSIFICATION OF THIS PAGE	19. SECURITY CLASSIFICATION OF ABSTRACT	20. LIMITATION OF ABSTRACT
Unclassified	Unclassified	Unclassified	Unlimited

NSN 7540-01-280-5500

Standard Form 298 (Rev. 2-89)
Prescribed by ANSI Std. Z39-18 298-102

USAPPC V1.00

FOREWORD

Opinions, interpretations, conclusions and recommendations are those of the author and are not necessarily endorsed by the U.S. Army.

MK Where copyrighted material is quoted, permission has been obtained to use such material.

MK Where material from documents designated for limited distribution is quoted, permission has been obtained to use the material.

MK Citations of commercial organizations and trade names in this report do not constitute an official Department of Army endorsement or approval of the products or services of these organizations.

____ In conducting research using animals, the investigator(s) adhered to the "Guide for the Care and Use of Laboratory Animals," prepared by the Committee on Care and Use of Laboratory Animals of the Institute of Laboratory Resources, National Research Council (NIH Publication No. 86-23, Revised 1985).

MK For the protection of human subjects, the investigator(s) adhered to policies of applicable Federal Law 45 CFR 46.

____ In conducting research utilizing recombinant DNA technology, the investigator(s) adhered to current guidelines promulgated by the National Institutes of Health.

____ In the conduct of research utilizing recombinant DNA, the investigator(s) adhered to the NIH Guidelines for Research Involving Recombinant DNA Molecules.

____ In the conduct of research involving hazardous organisms, the investigator(s) adhered to the CDC-NIH Guide for Biosafety in Microbiological and Biomedical Laboratories.

FOR Aug. 19, 1997

PI - Signature Date

RONALD B. SCHILLING

Table of Contents

List of Tables and Figures

INTRODUCTION

The goal of the research effort funded under this grant is to finalize the construction of two prototype DXM-1 slot-scanning digital mammography systems[1], conduct a technical evaluation of these prototypes and perform two clinical studies to assess the efficacy of the systems in the clinical environment. This program is scheduled to be completed during a 36 month effort.

The technical evaluation and one of the clinical studies is being conducted at the Radiology Department at the University of Arizona (UA) under the direction of Dr. Hans Roehrig. The objective of the technical evaluation is to determine system performance parameters such as dynamic range, modulation transfer function, sensitivity, etc. These parameters are to be measured and compared with film/screen performance characteristics. The objective of the clinical study conducted at UA is to acquaint and train radiologist to read digital mammograms from a monitor and to determine system efficacy in screening and diagnosis by imaging patients with known abnormal mammograms. One hundred women are scheduled to participate in this study.

The second clinical study was scheduled to be conducted at Sharp Healthcare/Sidney Kimmel Cancer Center in San Diego, California under the direction of Dr. Christine White. The objective of this study is to establish the clinical efficacy of the system compared with conventional film/screen mammography. One thousand women are scheduled to participate in this study.

The DXM-1 digital mammography system was designed and partially developed through funding obtained from the National Institutes of Health with two Small Business Inovative Research (SBIR) grants (phase I and phase II grant no. 2R44CA59104-02A1). Under these grants, the sensor chip technology was developed and an engineering prototype was produced which was used to acquire images of the Contrast Detail Mammography (CDMAM) phantom. These images established that the sensors are capable of acquiring superior quality images than conventional screen/film. Data acquired from these images was used to calculate the Detective Quantum Efficiency (DQE) and Modulation Transfer Function (MTF) for the prototype sensor array and is shown in Appendix A.

One result of the previous work was that it was determined that the original prototype sensors were not optimum for use in full-field mammography applications. A new sensor was designed incorporating several features including larger pixel size, larger active area on the sensor (i.e., more pixels) and an on-chip Time Delay and Integration (TDI) function. A camera and digital signal processor (DSP) was also designed during this effort.

Fisher Imaging Corporation, a subcontractor to this effort had previously developed a mammography gantry specifically designed for use with a digital slot-scanning imaging system using a different sensor technology. In connection with this effort Fisher will deliver two prototype gantries for use in the technical and clinical evaluation studies. One prototype has been delivered and is being modified. This unit will be used to conduct the technical evaluation. The second gantry will be delivered and used for the clinical evaluation later in the program.

The effort described above is broken down into three tasks: Integrate and Optimize the DXM-1 Mammography System; Engineering and Technical Evaluation; and Clinical Studies. The progress made to date for each of these tasks is discussed below.

TASK 1: DXM-1 Mammography System Integration

This task, scheduled to require nine months to complete has been delayed due to the necessity of redesigning the sensor chip and additional modifications required to the DSP unit. The sensor chips used in the DXM-1 were designed and fabricated in connection with previous work and were tested several months ago. The results obtained indicated that resolution was being degraded in the in-scan axis of the image. After subsequent analysis, it was determined that the chip design allowed for parasitic capacitance or charge sharing among the TDI summing capacitors on the sensor readout chip. In addition, the sensors produced in the last lot run had an extremely low yield such that only 2 working sensor were produced.

To correct these problems, the sensor chip was redesigned, a new mask set was generated and another lot run was initiated. This lot run is expected to be received by August 15, 1997. It is anticipated that these new sensor chips will show improved resolution and will be produced with sufficient yield to populate the two prototype systems required for this program.

The DSP unit required several modifications in order to operate at the desired speed (i.e., 10 Mhz) using a software implemented image formation algorithm. Since this has now been accomplished, two DSP units are being fabricated that utilize a firmware implemented image formation algorithm that will run at a speed of (20 Mhz). This higher operating speed is required in order to meet the goal of acquiring a full-field mammographic image in four seconds. It is anticipated that the firmware based DSP units will be received by September 15, 1997.

Despite the above mentioned problems, several images were acquired with the first prototype using only two of the required eight sensor chips. Although this system has only 1/4 of the total imaging area, several images were acquired and were analyzed. The data so produced has been used to complete the development of the system and make the required changes to the sensor chips and DSP unit. Several key parameters have been measured including: x-ray absorption efficiency, effective energy output of the x-ray generator and a preliminary noise analysis has been performed. In addition, some attempts have been made to generate a dark-substraction and flat-fielding algorithm while imaging the American College of Radiology (ACR) accreditation phantom. The ACR accreditation phantom is described in detail by DeParedes, et al[2], Hendrick, et al[3], and MeLelland, et al[4].

System parameters of the DXM-1 prototype were measured that primarily determine image quality. There are three areas of concern; the signal generation, the generation of noise and the removal of artifacts produced from the analog and digital signal processors.

The signal generation parameters measured are: x-ray absorption of the diode substrate material (silicon) and the effective energy of the x-ray generator. As shown in Figures B1 - B4, three detector substrates were placed in front of a phosphor-coated fiberoptic taper coupled to a Charge Coupled Device (CCD) camera. Images were acquired with this camera using an x-ray generator. Three different x-ray

spectra were used to obtain these images: 80 kVp, 30 kVp and 26 kVp. Using specific filters in connection with these spectra, a well characterized effective x-ray energy is produced. For the 80 kVp spectra, the effective energy is 50.5 keV, for the 30 kVp spectra, 19 keV and 14.9 keV for the 26 kVp spectra. The total absorption measured with these energies is shown in the table below and compared with data calculated from first principles:

Effective X-ray Energy	Calculated Absorption	% Absorption (1.53mm of Si)
50.5 keV	14%	12.3%
19 keV	76%	73.3%
14.9 keV	96%	86.9%

These data suggest that an absorption efficiency of 73 to 86% can be expected for typical mammography spectra using a 1.53 mm silicon detector substrate. These values correlate well with the calculated values. The calculated values assume a monoenergetic, collimated beam of x-rays.

The x-ray generator that will be used in connection with this study was characterized to determine its effective energy at two energy settings, with and without an absorber (to simulate tissue). The effective energy was determined as described by Johns and Cunningham[5] and by Hillen, et al[6]. The results of this study are shown in Figures B5 - B7 and are summarized in the table below:

Energy Spectra	No Absorber	3.9 cm Plexiglass
26 kVp	14.89 keV (E-eff)	18.73 keV (E-eff)
30 kVp	15.55 keV (E-eff)	17.99 keV (E-eff)

These data show that the effective energy of the generator is approximately half of the peak tube voltage with no absorber. The effective energy is increased by beam hardening through the plexiglass absorber. Accordingly, the absorption efficiency of the detector substrate will decrease from 87% to 73% with a 26kVp spectra due to absorption and beam hardening in the breast tissue.

Three parameters that affect the performance of the DXM-1 imager were measured: Mean and Standard Deviation, Signal-to-Noise Ratio (SNR), noise power spectrum (NPS) and dark signal generation. To analyze the Mean and Standard Deviation, the mean analog-to-digital units (ADU) were measured and plotted vrs relative exposure in mA. These measurements were made by acquiring x-ray images with the DXM-1. An area of interest (AOI) was selected in the image containing approximately 10,000 pixels. Each pixel consists of a gray-level value produced by the digitized TDI sum of the detector elements on the sensor array. Each pixel contains a 16-bit digital word to represent its gray level value, thus each pixel has a capacity of 16,384 ADUs or gray levels. It is important to note that the Mean increases linearly with exposure.

The DXM-1 sensor arrays contain two separate banks of detectors off-set by half a pixel in the in-scan and cross-scan direction. Results obtained with both banks of sensors were plotted as shown in Figure B8. As shown bank 2 consistently has a higher sensitivity than bank 1 and both banks show an increased output as exposure is increased. The root-mean square (RMS) of the ADU was plotted vrs exposure for both banks of sensors and is shown in Figure B9. Note that the RMS increases as the square root of the exposure. The Signal-to-Noise Ratio (SNR) calculated by dividing the mean with the RMS, is plotted vrs exposure in Figure B10. As shown, the SNR is about 45:1 at an exposure of 25 mA and increases with increasing exposure to about 85:1 at an exposure of 130 mA. Also note that the SNR increases as the square root of the exposure as well.

The Mean (ADU) of the sensor array AOI was measured without x-ray exposure as a function of time for both banks of sensors. The results are shown in Figure B11. As shown, the mean dark signal increases as a function of time for both banks of sensors. Bank 1 has a higher dark current generation rate than Bank 2. The increase in dark current generation is attributed to the temperature rise experienced by the camera and sensor array due to heat generated while the system is on.

The noise power spectrum (NPS) of the sensor arrays was determined as described by Dainty, et al[7] and Roehrig, et al[8] and is plotted as a function of frequency from 0 to 10 line pairs/mm (lp/mm). Data was obtained with and without x-ray exposure. The results of this study are shown in Figures B12 and B13. As shown in Figure B12, the NPS of both banks of sensors decreases slightly as frequency increases for both cases (with and without x-ray exposure). As shown in Figure B13, the NPS was obtained under four exposure conditions with the accreditation phantom. The NPS decreases with increased exposure and frequency.

Images were acquired of the accreditation phantom to characterize the amount of fixed pattern noise and other artifacts created by the camera and DSP system. Images obtained are shown in Figures B14 and B15. A schematic of the accreditation phantom is shown in Figure B16. As shown in Figure B14, at an exposure of 75 mA, mass groups 13 - 15 are visible, while 16 is not. Figure B15 shows the same mass groups taken at an exposure of 100 mA. At this exposure mass group 16 is not visible either. These images were produced with a dark-subtraction and flat-fielding algorithm applied to the raw image data.

Another task yet to be completed is the development of the image restoration software and user interface software. These programs will be used by the radiologist to clean up the image data to remove scanning artifacts and pixel induced artifacts and to allow the radiologist to set up and control the image acquisition sequence. It is anticipated that these programs will be completed by September 30, 1997.

TASK 2: Engineering and Technical Evaluation of the DXM-1 System

This task scheduled to begin in April, 1997 has been delayed due to the problems encountered in task 1. However, some preliminary data is being produced utilizing the images acquired with the existing version of the prototype. These data are not yet available for reporting purposes. It is anticipated that this task will delayed until October 1, 1997.

TASK 3: Clinical Studies to Assess Efficacy of the DXM-1 Digital Mammography System

Recently, the principal investigator for the clinical trial program subcontracted to Sharp Healthcare, Dr. Christine White, left her position there. One of her colleagues, Dr. Linda Olson is a professor at the University of California at San Diego (UCSD). She has agreed to become the principal investigator for the clinical trial program and run it through the university hospital.

A request for a change of venue was made for the clinical trial program in connection with this effort from Sharp Healthcare to UCSD on June 13, 1997. A reply was received requesting a protocol, IRB approval, safety program and patient informed consent form from UCSD, a CV from Dr. Olson and a redirection of funds budget. These items were forwarded to the MCMR grants office on June 30, 1997. We are waiting final approval to transfer the clinical trial program to UCSD.

The revised clinical trial program is proposed to begin on January 1, 1998. The scope of work proposed is essentially identical to the original trial and the proposed budget will not change the current level of funding for this grant.

Conclusions

Overall progress to date on this effort has been delayed due to technical difficulties in the DXM-1 system integration. Moreover, one of the clinical trial venues needs to be changed due to the departure of the program director at the originally chosen facility. This has resulted in a slippage in milestone performance of six to twelve months in some cases. However, much of this lost time can be made up during the next six months if our contractors perform as anticipated.

Some conclusions can be made at this time based on the preliminary data gathered thus far on the DXM-1 system. The system response is linear with exposure dose and it appears that the dominant noise source is quantum (x-ray) noise. Efforts are now underway to improve system performance by removing artifacts generated in the image reconstruction process, to eliminate parasitic capacitance on the readout IC, and to increase resolution by interleaving both banks of sensors into the displayed image.

During the next reporting period a significant amount of technical and clinical data will be generated in connection with this program. Preliminary findings indicate that the primary objective of this effort, the demonstration of a new imaging technology that has superior performance to conventional screened film will be established. Of particular importance is the fact that through this program, significant clinical and technical data will be generated that will greatly enhance the viability of this technology and will greatly expedite the transition of this technology in to the clinical environment.

References

1. Cox, J.D., Sharma, S.R., and Schilling, R.B., "Advanced Digital Mammography", Proceedings of the Annual Meeting of the Society for Computer Applications in Radiology (SCAR), June 21-24, 1997, Rochester Minnesota.

2. DeParedes ES, Frazier AB, Hartwell GD, et al: Development and implementation of a quality assurance program for mammography. Radiology 163:83-85, 1987.

3. Hendrick RE: Standardization of image quality and radiation dose in mammography. Radiology 174:648-654, 1990

4. McLelland R, Hendrick RE, Zinninger MD, Wilcox PA: The American College of Radiology Mammography Accreditation Program" AJR 157:473-479, 1991

5. Harold Elford Johns and John Robert Cunningham, "The Physics of Radiology." Third Edition, Seventh printing, Charles C. Thomas - Publisher, Springfield, Illinois, 1974.

6. Hillen, W., U. Schiebel, and T.Zaengel, "Imaging performance of a digital storage phosphor system," Med. Phys., 1987;14(5):744.

7. Dainty, J.C., and R. Shaw, "Image Science; principles, analysis and evaluation of photographic-type imaging processes", Academic Press, London, New York, San Francisco, (1974).

8. Roehrig H, Schempp, W, Fajardo LL, Yu T: "Signal, noise and Detective Quantum Efficiency in CCD based x-ray imaging systems for use in mammography" Proc. SPIE Vol 2163, 320-332,(1994)

Appendix A

Primary Slot Scan System DQE is About 10x Better Than Film–screen

- Quantum efficiency of a 1.5mm detector is over 80%.
- Scatter and grid effects reduce system DQE of film–screen to about 7%.

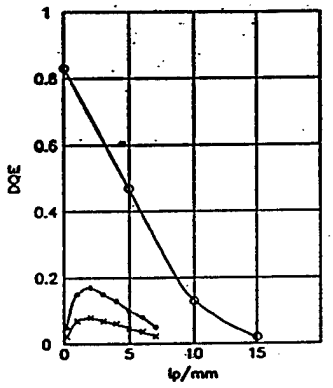

• – DQE of Kodak MIN–R Screen/Ortho–M Film
o – DQE of 1.5mm Thick PrimeX Detector
× – System DQE of Film/Screen With Scatter Grid

Ref: "Detective quantum efficiency of selected mammographic screen–film combinations." In: Medical Imaging III: Image Formation, SPIE 1090, 1989: p72–74

Modulation Transfer Function Data Approaches Predicted Values

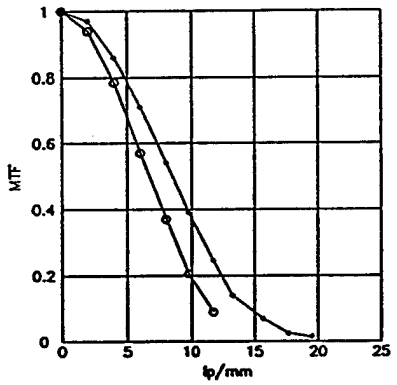

• – MTF of 1mm Detector (2 Samples per Dwell)
o – MTF of 1mm Detector (1 Sample per Dwell)

Experimental DQE Data Consistent With Predictions

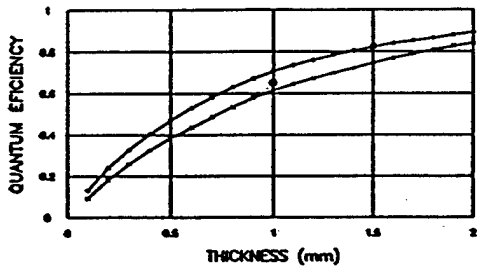

o – Measured DQE
• – Predicted DQE (W Target X–ray Spectra)
• – Predicted DQE (Mo Target X–ray Spectra)

Figure A–1

Appendix B

X-ray Absorption of the 1.53 mm thick Silicon of the Primex x-ray converter.

Primex Si-detector; absorption of x-rays, estimated from x-ray images of three detector pieces, placed on the input of a CCD-based x-ray camera, using a screen fiber-optically coupled to the 1024 x 1024 pixel CCD. The x-ray camera had a field of view of about 5 cm x 5 cm. The enclosed schematic describes the experimental set-up.

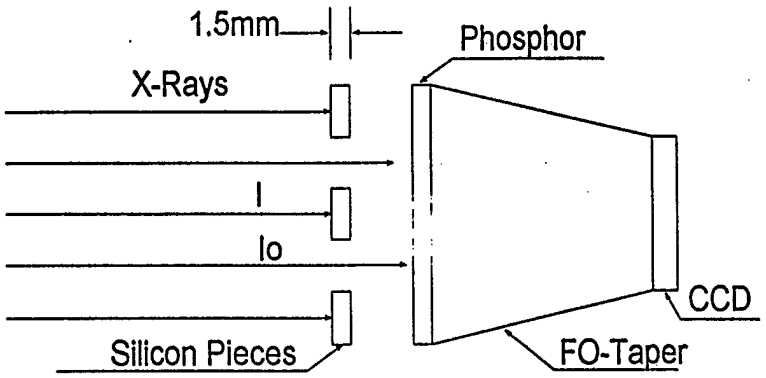

The idea was to determine the absorption A from the measurements of Signal (equivalent to I) and Background (equivalent to I_o) as

$A = (I_o - I)/I_o$ = (Background - Signal)/Background

The enclosed three figures are sample images for the three x-ray conditions A., B., and C. The profiles show how the digital values for Signal (= I) and Background (= I_o) were determined

The result of the measurements:

At 50.5 keV effective energy (HVL = 7.21 mm Al), using a CGR source at 80 kVp + 20 mm Al
Absorption : 12.3%

At 19 keV effective energy (HVL = 0.655 mm Al), using a Toshiba "Mammo-Source", at 30 kVp + 3.9 cm Plexiglass
Absorption overall: 73.3%

At 14.9keV effective energy (HVL = 0.339 mm Al), using a Toshiba "Mammo-Source", at 26 Kvp and Mo-Filter
Absorption : 86.9%

Figure B-1

Primex detector on CCD camera with optical fiber reducer
X-ray Source: 80Kvp, 2 cm Al(50Kev)

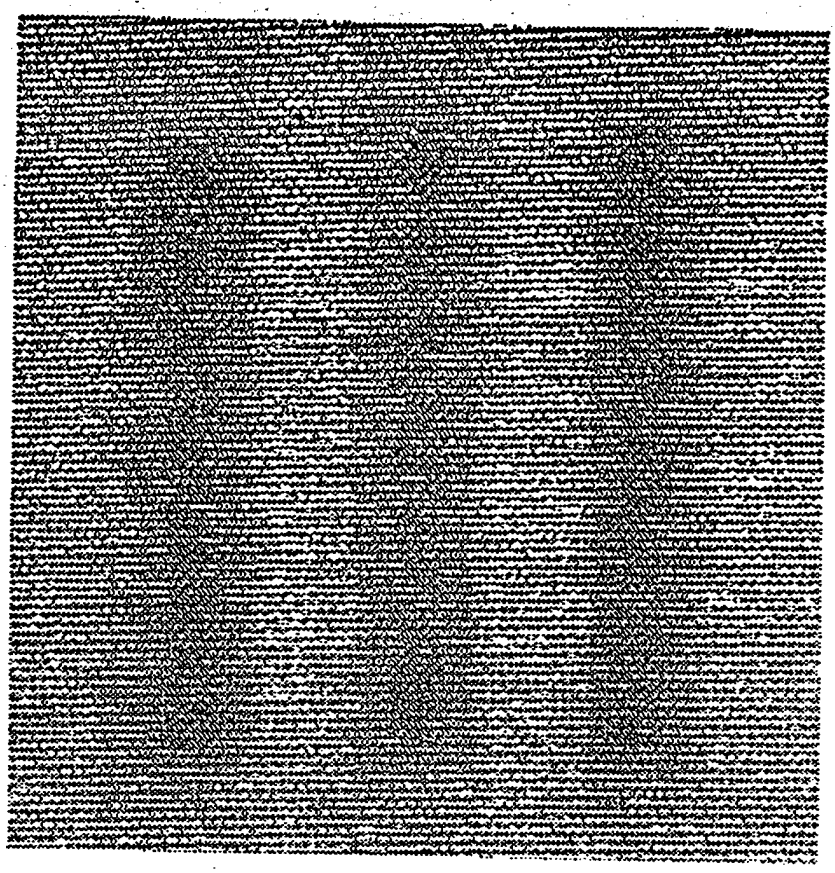

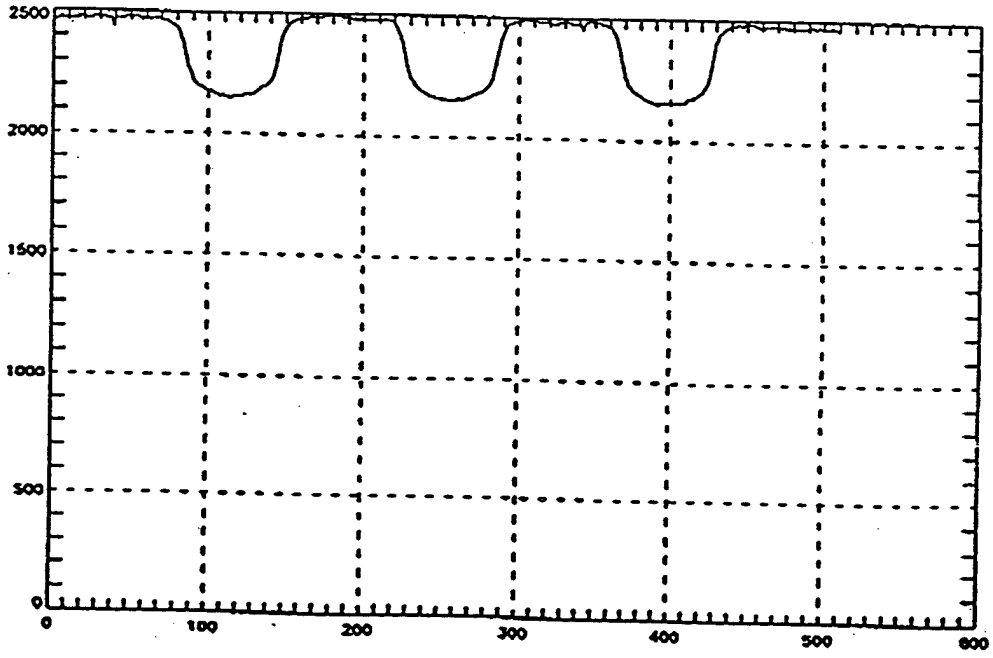

Figure B-2

Primex detector on CCD camera with optical fiber reducer
X-ray Source: 30 Kvp, Plus plexiglass filer(20Kev)

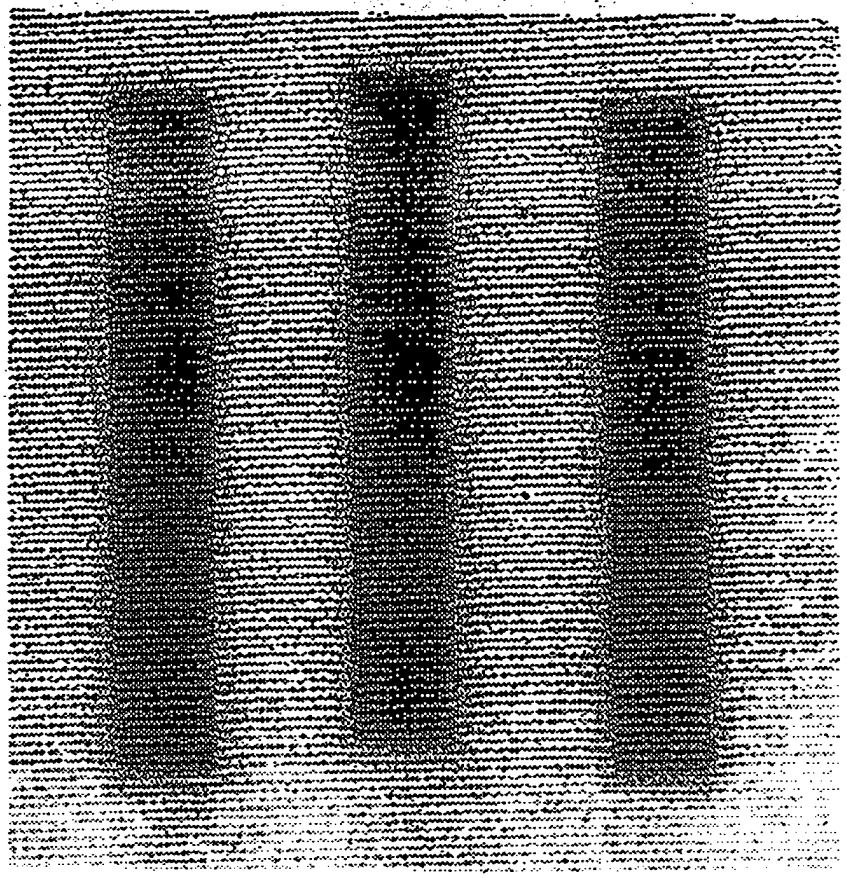

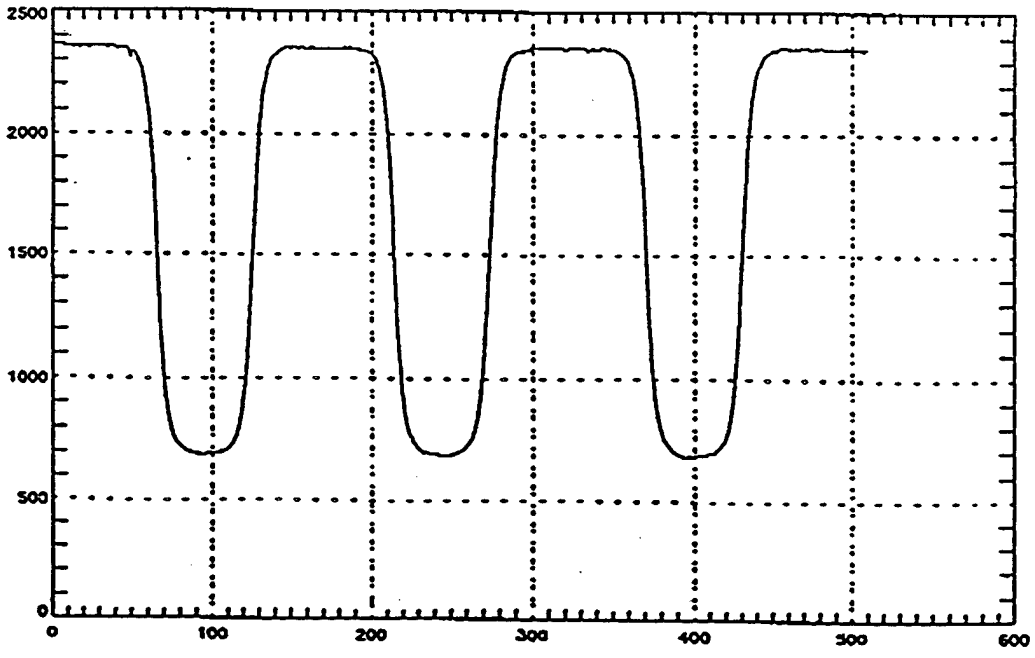

Figure B-3

Primex detector on CCD camera with optical fiber reducer
X-ray Source: 26 Kvp, no X-ray filter

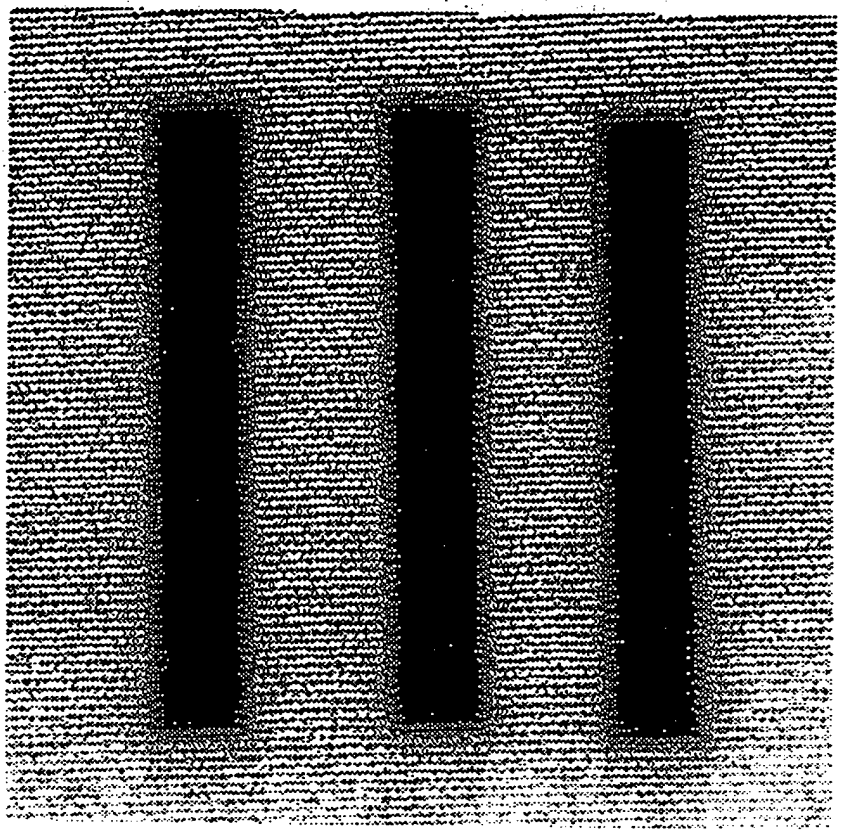

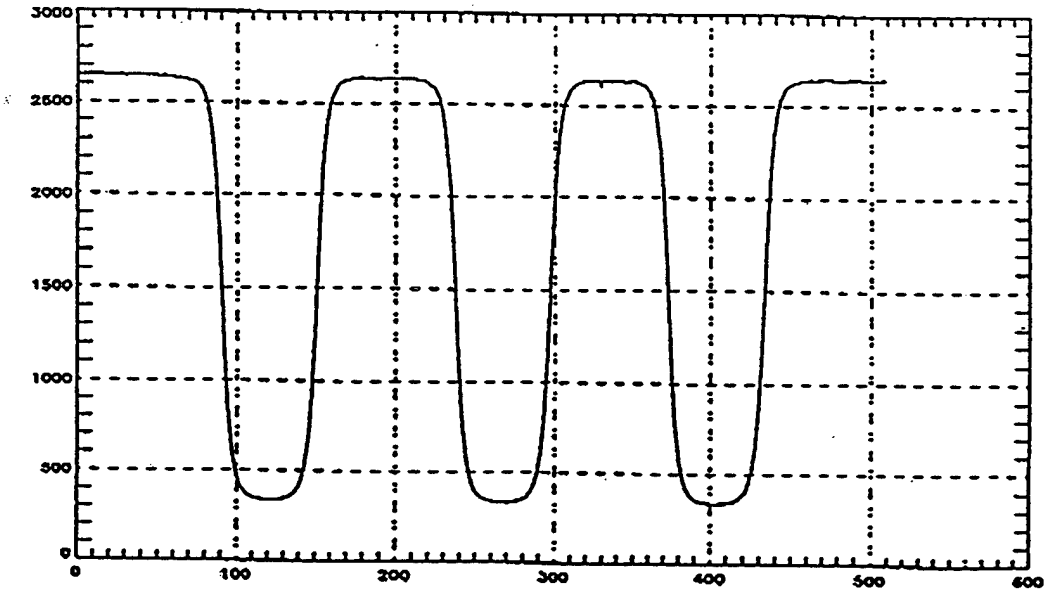

Figure B-4

The size of each of the three detector pieces was approximately

	Object 1	Object 2	Object 3
length [mm]:	18.84	18.88	18.84
width [mm]:	2.84	2.85	2.83
height [mm]:	1.53	1.52	1.52
Volume [cm^3]	.082	.082	.081
Weight [g]	.18865	.18865	.18815
Density [g/cm^3]	2.301	2.301	2.323
Density of Si from reference books [g/cm^3]	2.42	2.42	2.42

A.: Exposures at 50.5 keV effective energy (HVL = 7.21 mm Al),using CGR source at 80 kVp + 20 mm Al

Exposure	Pos.	Object 1				Object 2				Object 3			
		Signal	Back-ground	Diff.	Absorption	Signal	Back-ground	Diff.	Absorption	Signal	Back-ground	Diff.	Absorption
1.	1.	1011	1153	142	.123	1016	1157	141	.122	1009	1154	145	.126
	2.	1016	1155	139	.120	1015	1161	146	.126	1014	1159	145	.126
	3.	1011	1158	147	.127	1015	1159	144	.124	1011	1155	144	.124
Absorption, ave:					12.3%				12.4%				12.5%
2.	1.	2122	2430	308	.127	2128	2436	308	.126	2125	2423	298	.123
	2.	2129	2434	305	.125	2134	2444	310	.127	2139	2428	289	.119
	3.	2125	2427	302	.124	2129	2437	308	.126	2126	2433	307	.126
Absorption, ave:					12.5%				12.6%				12.3%
3.	1.	2903	3295	392	.119	2898	3303	405	.123	2898	3299	401	.122
	2.	2904	3298	394	.119	2911	3307	396	.120	2899	3308	409	.124
	3.	2898	3291	393	.119	2900	3306	406	.123	2901	3297	396	.120
Absorption, ave:					11.9%				12.2%				12.2%

Absorption overall: 12.3%

Figure B-5

B.: Exposures at 19 keV effective energy (HVL = 0.655 mm Al), using a Toshiba "Mammo-Source", at 30 kVp + 3.9 cm Plexiglass

Exposure	Pos.	Object 1				Object 2				Object 3			
		Signal	Back-ground	Diff.	Absorption	Signal	Back-ground	Diff.	Absorption	Signal	Back-ground	Diff.	Absorption
1.	1.	562	2142	1580	.738	562	2141	1579	.738	568	2139	1571	.734
	2.	557	2146	1589	.740	557	2141	1584	.740	566	2139	1573	.735
	3.	556	2144	1588	.741	561	2138	1577	.738	563	2144	1581	.737
Absorption, ave:					74.0%				73.9%				73.5%
2.	1.	940	3439	2499	.727	934	3432	2498	.728	946	3430	2484	.724
	2.	932	3445	2513	.729	932	3432	2500	.728	942	3428	2486	.725
	3.	931	3433	2502	.729	936	3434	2498	.727	939	3428	2489	.726
Absorption, ave:					72.8%				72.8%				72.5%

Absorption overall: 73.3%

C.: Exposures at 14.9keV effective energy (HVL = 0.339 mm Al), using a Toshiba "Mammo-Source", at 26 Kvp and Mo-Filter

Exposure	Pos.	Object 1				Object 2				Object 3			
		Signal	Back-ground	Diff.	Absorption	Signal	Back-ground	Diff.	Absorption	Signal	Back-ground	Diff.	Absorption
1.	1.	249	1927	1678	.870	247	1916	1669	.871	252	1926	1674	.869
	2.	245	1924	1679	.873	243	1916	1673	.873	246	1924	1678	.872
	3.	244	1924	1680	.873	245	1919	1674	.872	247	1923	1676	.872
Absorption ave:					87.2%				87.2%				87.1%
2.	1.	475	3540	3065	.866	471	3527	3056	.866	478	3540	3062	.865
	2.	465	3543	3078	.865	462	3532	3070	.869	468	3543	3075	.868
	3.	466	3550	3084	.869	471	3544	3073	.867	476	3541	3065	.866
Absorption ave:					86.7%				86.7%				86.6%

Absorption overall: 86.9%

Figure B-6

Half-Value layers of Primex Mammo-x-source

3.9 cm Plexiglass		3.9 cm Plexiglass	No Plexiglass	No Plexiglass
Al-Thickn [mm]	[30 kVp] Exposure [mr]	[26 kVp] Exposure [mr]	[30 kVp] Exposure [mr]	[26 kVp] Exposure [mR]
0	79.6	37.8	2790	1771
0.1	70.6	33.9	2220	1374
0.2	63.2	29.3	1826	1095
0.3	56.56	26	1523	899
0.4	50.5	22.6	1276	742
0.5	45	20.05	1094	621
0.6	40.75	17.9	920	519
0.7	36.4	15.65	779	
0.8	32.9	13.95		
0.9	29.8	12.5		
1	27	11.02		
	HVL: 0.626 mm Al	HVL 0.557 mm Al	HVL 0.363 mm Al	HVL 0.32 mm Al
	mu/rho (0.5) 4.101	mu/rho (0.5) 4.609	mu/rho (0.5) 7.0722	mu/rho (0.5) 8.0225
	E-eff [kev] 18.73	E-eff [keV] 17.99	E-eff [keV] 15.55	E-eff [keV] 14.89

Figure B-7

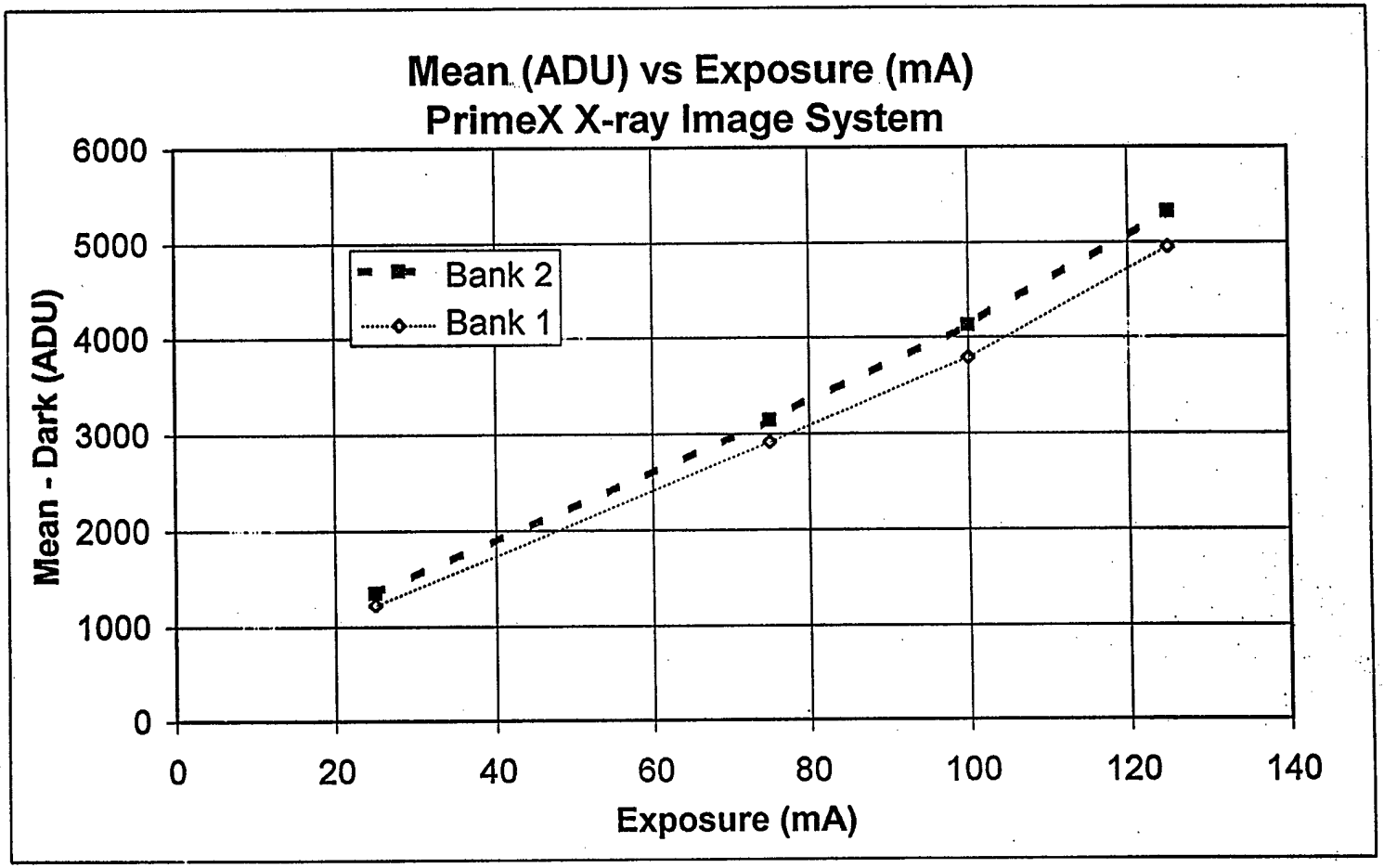
Mean (ADU) vs Exposure (mA)
PrimeX X-ray Image System
Mean - Dark (ADU)
6000
5000
4000
3000
2000
1000
0
Bank 2
Bank 1
0
20
40
60
80
100
120
140
Exposure (mA)

Figure B-8

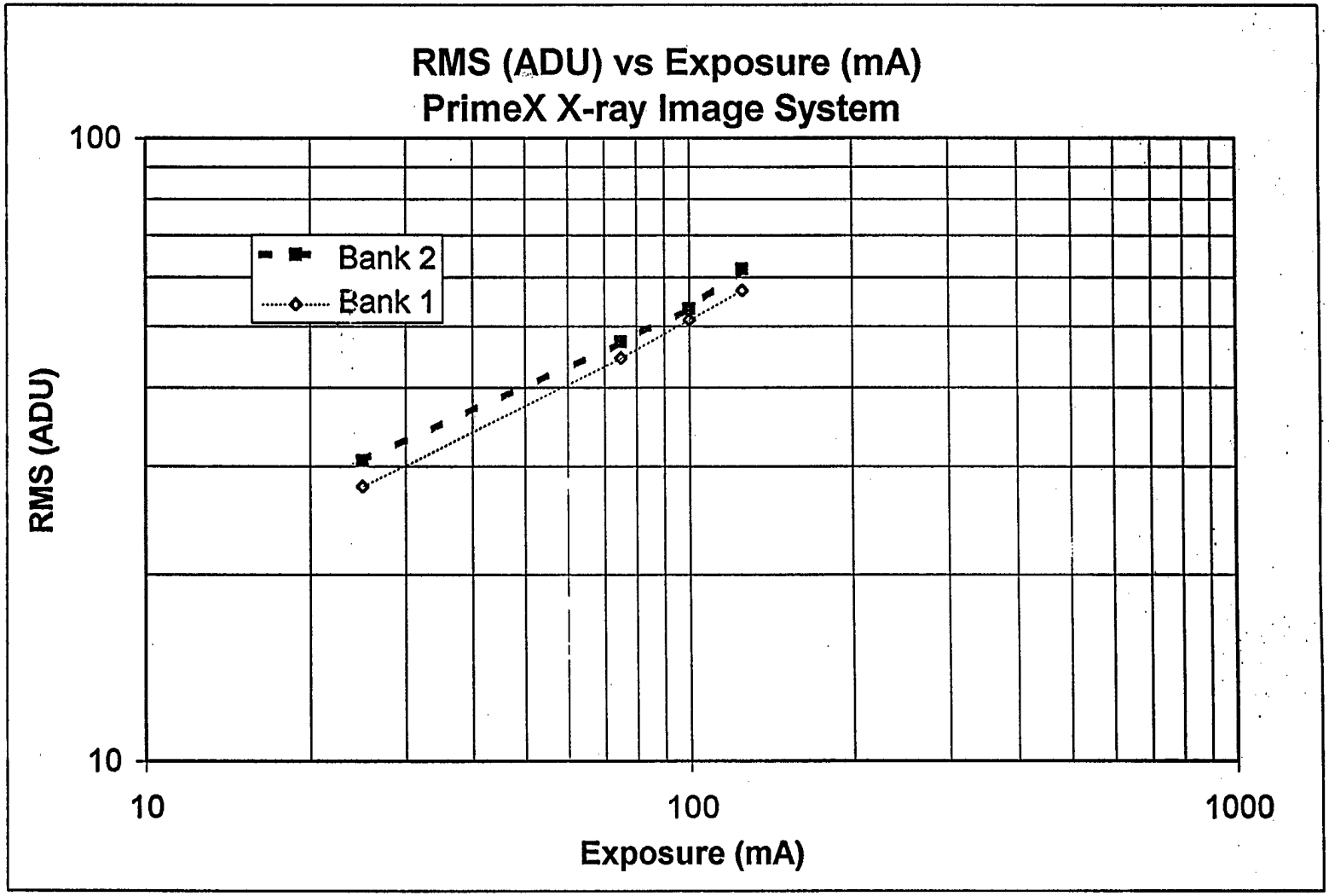
RMS (ADU) vs Exposure (mA)
PrimeX X-ray Image System
100
10
RMS (ADU)
Bank 2
Bank 1
10
100
1000
Exposure (mA)

Figure B-9

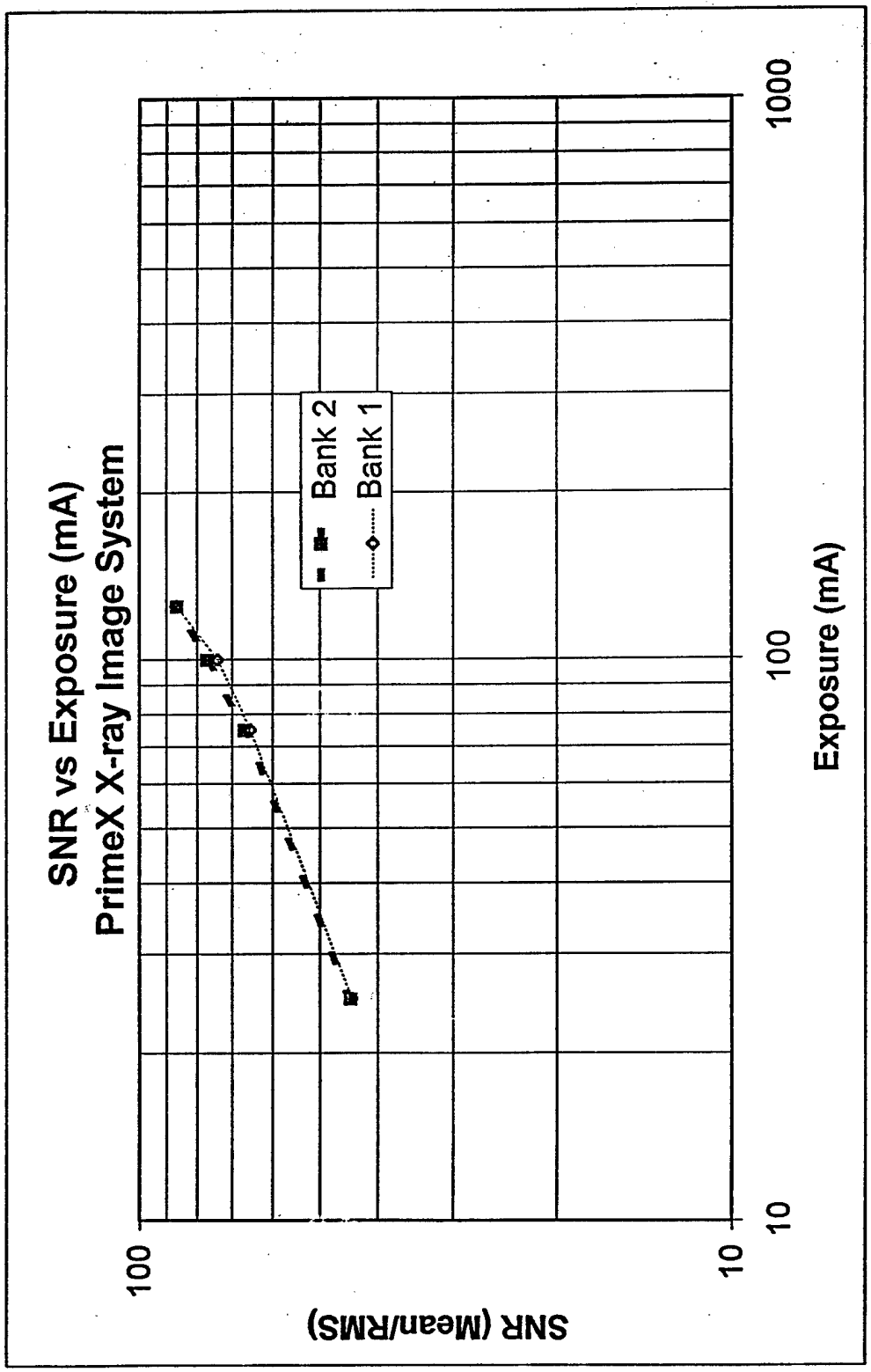
SNR vs Exposure (mA)
PrimeX X-ray Image System
Bank 2
Bank 1
SNR (Mean/RMS)
100
10
10
100
1000
Exposure (mA)

Figure B-10

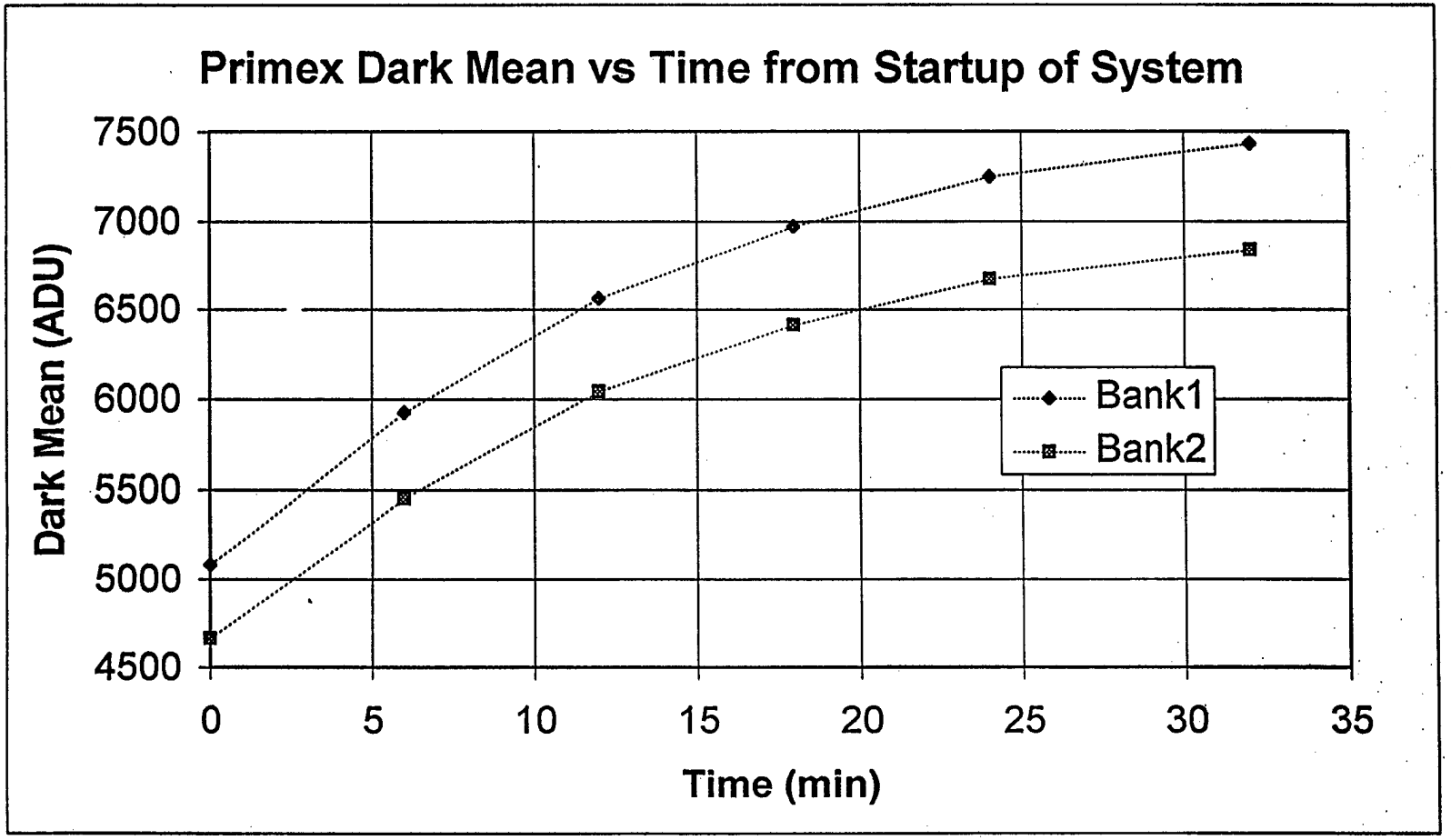
Primex Dark Mean vs Time from Startup of System
Dark Mean (ADU)
7500
7000
6500
6000
5500
5000
4500
0
5
10
15
20
25
30
35
Time (min)
Bank1
Bank2

Figure B-11

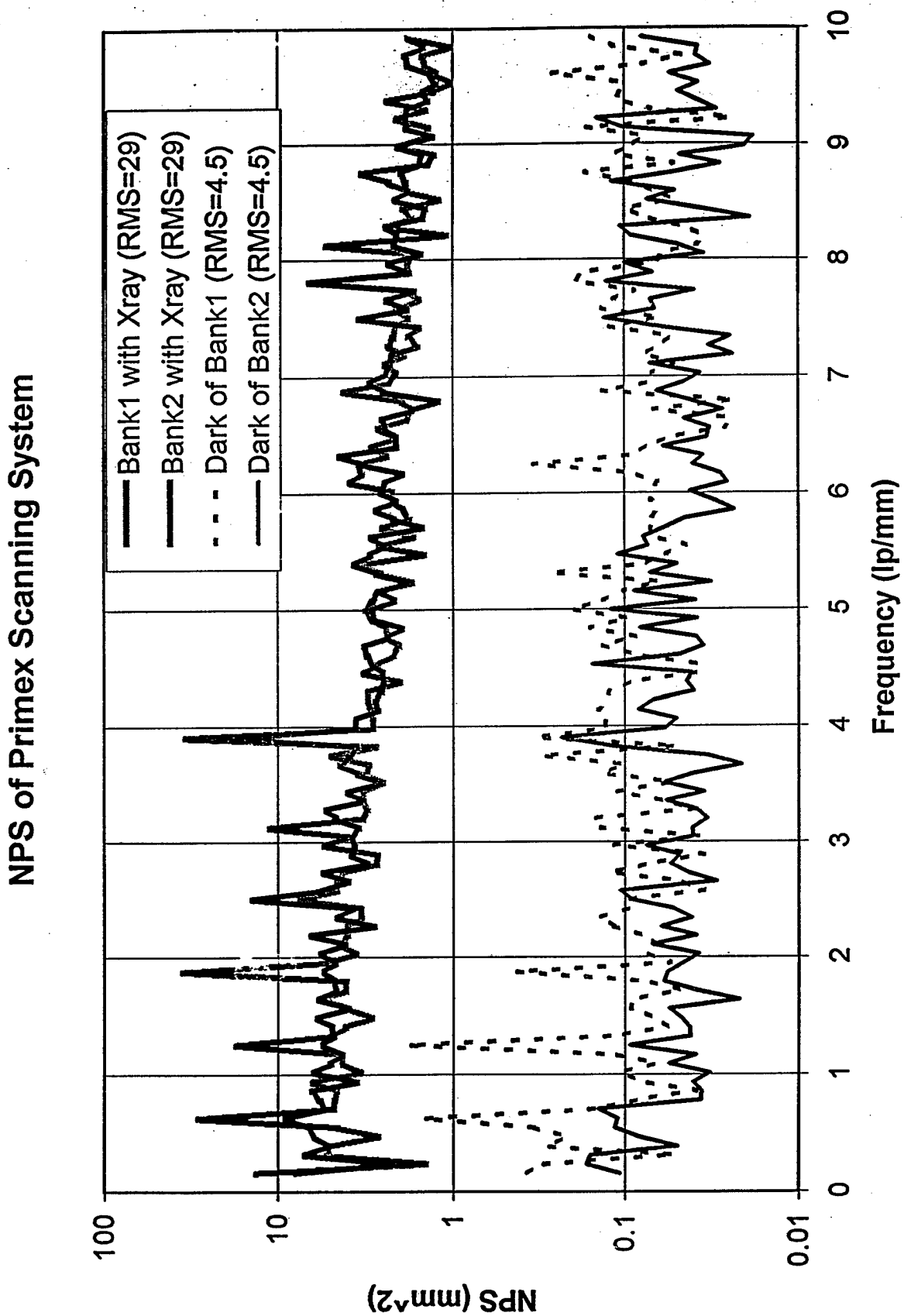
NPS of Primex Scanning System
Bank1 with Xray (RMS=29)
Bank2 with Xray (RMS=29)
Dark of Bank1 (RMS=4.5)
Dark of Bank2 (RMS=4.5)
NPS (mm^2)
100
10
1
0.1
0.01
0
1
2
3
4
5
6
7
8
9
10
Frequency (lp/mm)

Figure B-12

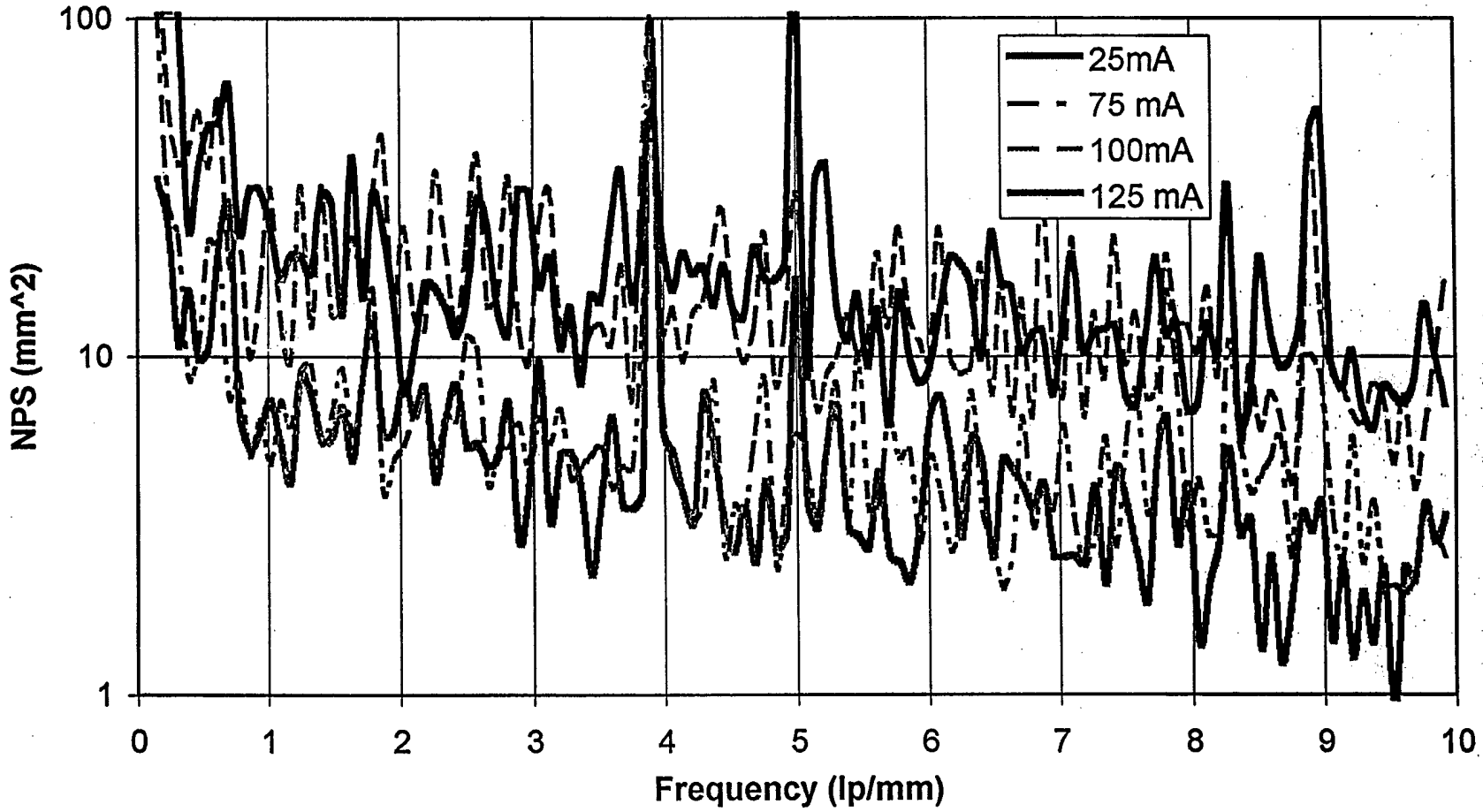
NPS of Primex System
100
10
1
NPS (mm^2)
0
1
2
3
4
5
6
7
8
9
10
Frequency (lp/mm)
25mA
75 mA
100mA
125 mA

Figure B-13

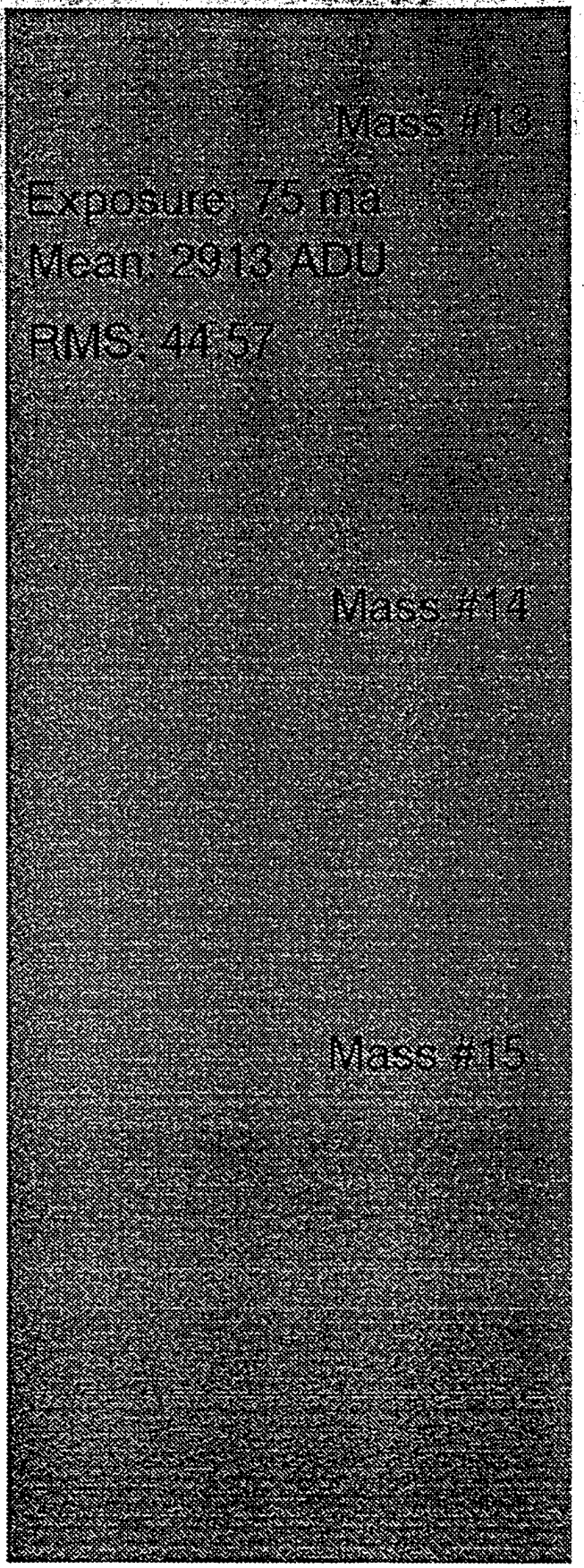

Figure B-14

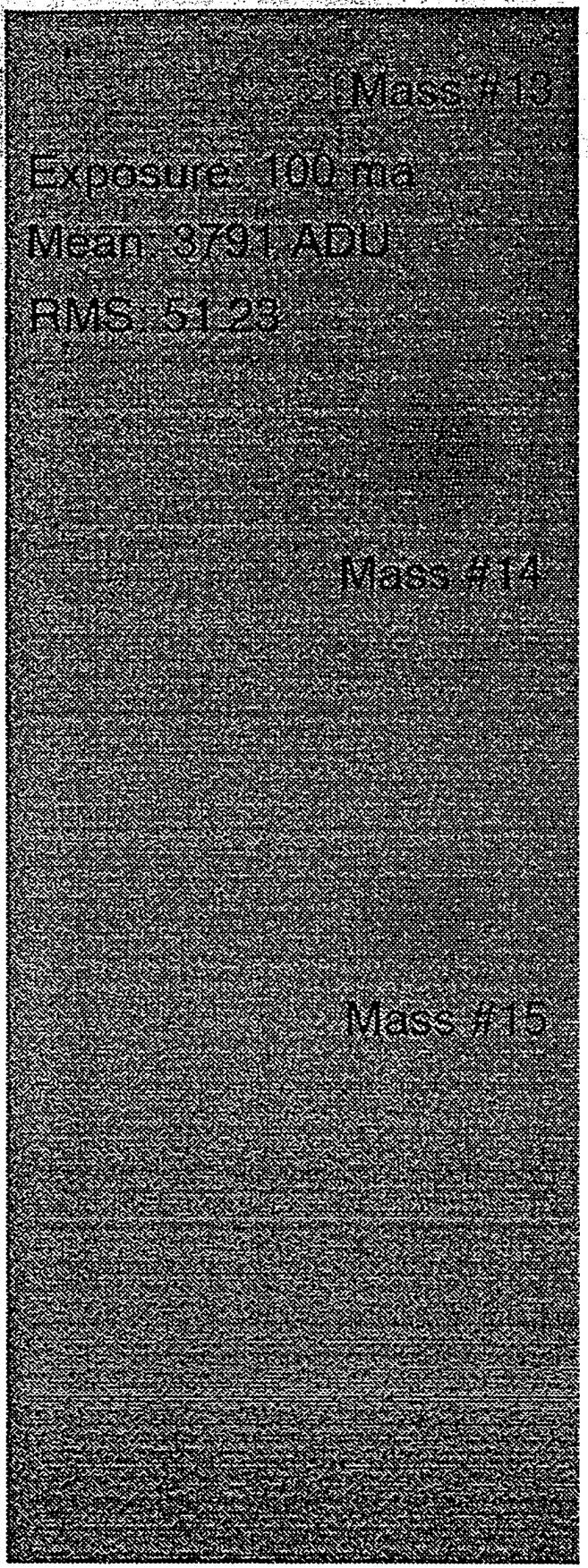

Figure B-15

2. DESCRIPTION

The Mammographic Phantom is made up of a wax block containing 16 various sets of test objects, a 3.3 cm (1.3 inch) thick acrylic base, a tray for placement of the wax block, and a .3 cm (.12 inch) thick cover. All of this together approximates a 4.0 to 4.5 cm compressed breast. Five simulated micro-calcifications, six different size nylon fibers simulate fibrous structures, and five different size tumor-like masses are included in the wax insert.

Figure 2 lists the sizes of the test objects and their position in relation to the notched corner of the wax block.

	Region Materials
1.	1.56 mm nylon fiber
2.	1.12 mm nylon fiber
3.	0.89 mm nylon fiber
4.	0.75 mm nylon fiber
5.	0.54 mm nylon fiber
6.	0.40 mm nylon fiber
7.	0.54 mm simulated micro-calcification
8.	0.40 mm simulated micro-calcification
9.	0.32 mm simulated micro-calcification
10.	0.24 mm simulated micro-calcification
11.	0.16 mm simulated micro-calcification
12.	2.00 mm tumor-like mass
13.	1.00 mm tumor-like mass
14.	0.75 mm tumor-like mass
15.	0.50 mm tumor-like mass
16.	0.25 mm tumor-like mass

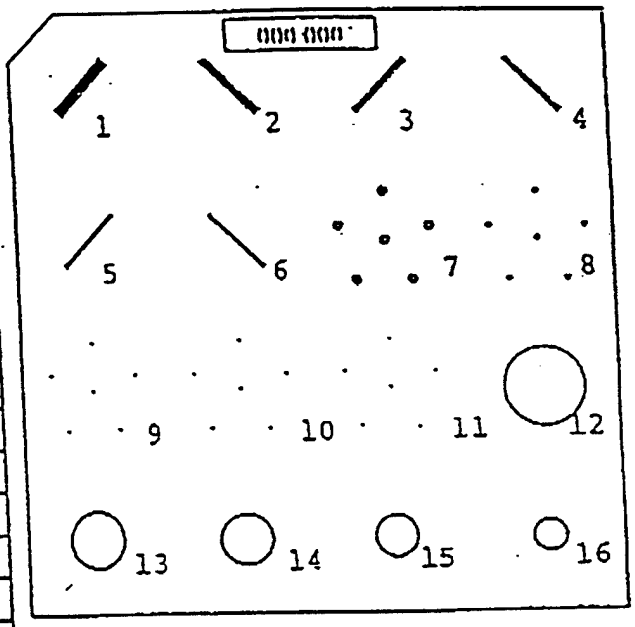

Figure 2. A schematic view of the Mammographic Phantom giving the test object sizes and position numbers used for reference.

> ***Note:*** *Numbers are for reference only. The wax block can be removed (carefully) and placed in different orientations (even upside down) for a randomized effect if desired.*

Figure B-16